Acta Crystallographica Section F
Structural Biology and Crystallization Communications
ISSN 1744-3091

Expression, purification, crystallization and preliminary X-ray analysis of the DNA-binding domain of *Rhodobacter capsulatus* MopB

Alexandra Müller,[a] Christine Schlicker,[b] Maria Fehringer,[a] Bernd Masepohl[a] and Eckhard Hofmann[b]*

[a]Lehrstuhl für Biologie der Mikroorganismen, Fakultät für Biologie und Biotechnologie, Ruhr-Universität Bochum, 44780 Bochum, Germany, and [b]Lehrstuhl für Biophysik, Fakultät für Biologie und Biotechnologie, Ruhr-University Bochum, 44780 Bochum, Germany

Correspondence e-mail: eckhard.hofmann@bph.ruhr-uni-bochum.de

Received 16 November 2010
Accepted 30 December 2010

The LysR-type regulator MopB represses transcription of several target genes (including the nitrogen-fixation gene *anfA*) in *Rhodobacter capsulatus* at high molybdenum concentrations. In this study, the isolated DNA-binding domain of MopB ($MopB_{HTH}$) was overexpressed in *Escherichia coli*. Purified $MopB_{HTH}$ bound the *anfA* promoter as shown by DNA mobility-shift assays, demonstrating the function of the isolated regulator domain. $MopB_{HTH}$ was crystallized using the sitting-drop vapour-diffusion method in the presence of 0.2 *M* lithium sulfate, 0.1 *M* phosphate/citrate pH 4.2, 20%(*w*/*v*) PEG 1000 at 291 K. The crystal belonged to space group $P3_121$ or $P3_221$, with unit-cell parameters $a = b = 61.84$, $c = 139.64$ Å, $\alpha = \beta = 90$, $\gamma = 120^\circ$, and diffracted to 3.3 Å resolution at a synchrotron source.

1. Introduction

Members of the LysR-type transcription regulator (LTTR) family are widely distributed within bacteria and archaea. LTTRs control diverse cellular processes such as virulence, CO_2 fixation, quorum sensing and nitrogen assimilation (Viale *et al.*, 1991; Schlaman *et al.*, 1992; Schell, 1993; Cao *et al.*, 2001; Russell *et al.*, 2004; Bender, 2010). These regulators typically consist of an N-terminal DNA-binding domain with a helix–turn–helix motif and a C-terminal effector-binding domain. LTTRs bind to conserved palindromic sequences called LTTR boxes within their target promoters. The minimal consensus sequence of LTTR boxes is T-N_{11}-A (Parsek *et al.*, 1994). LTTRs mostly form dimers and can both activate and repress the expression of target genes depending on the position of the LTTR box relative to the transcription start site (Maddocks & Oyston, 2008). Binding of LTTRs to target promoters is modulated by different effectors, which can be either metabolites or extracellular factors. Effector binding to the C-terminal domain results in conformational changes that control the affinity of the N-terminal domain for the respective target promoter (Schell, 1993).

Rhodobacter capsulatus is a free-living phototrophic bacterium that is known for its high metabolic versatility (Madigan, 1995). In the absence of ammonium, *R. capsulatus* reduces atmospheric dinitrogen to ammonia *via* two nitrogenases: a molybdenum-containing nitrogenase (Mo-nitrogenase) and a molybdenum-free alternative iron-only nitrogenase (Fe-nitrogenase). Fe-nitrogenase, which exhibits a lower specific activity than Mo-nitrogenase, is only synthesized in the absence of molybdate (Masepohl & Hallenbeck, 2010). In the presence of molybdate the dimeric regulator MopB represses the transcription of *anfA*, which codes for the transcriptional activator of Fe-nitrogenase genes (Kutsche *et al.*, 1996; Wiethaus *et al.*, 2006). The *anfA* promoter region encompasses a specific LTTR-box (Mo-box) which overlaps the transcription start site. The affinity of MopB for the *anfA* Mo-box is increased upon binding of molybdate (Wiethaus *et al.*, 2006). MopB exhibits 32% sequence identity to the LTTR-like regulator ModE from *Escherichia coli* (Anderson *et al.*, 1997). The crystal structures of ModE and a few other LTTRs have been solved, revealing the exact modular organization of the proteins as well as the conformational changes upon effector binding (Hall *et al.*, 1999;

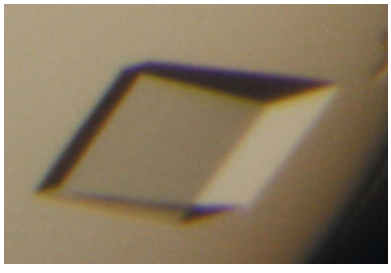

Muraoka *et al.*, 2003; Zaim & Kierzek, 2003; Monferrer *et al.*, 2010). In the present study, we demonstrate that the isolated DNA-binding domain of MopB ($MopB_{HTH}$) retains full binding activity for the *anfA* promoter. $MopB_{HTH}$ was crystallized and preliminary X-ray analyses were carried out.

2. Experimental procedures

2.1. Overexpression and purification of $MopB_{HTH}$

A DNA fragment coding for the DNA-binding domain of MopB (RRC03910; http://www.ergo-light.com; Fig. 1; amino acids 1–120) was PCR-amplified using the primer pair 5′-ATACATATGAC-GGACGGTGTG-3′ and 5′-GTGCTCGAGGGACAGACC-3′ with *R. capsulatus* chromosomal DNA as template. The PCR product was digested with *Nde*I and *Xho*I and ligated into vector plasmid pET22b (Novagen). The resulting hybrid plasmid coding for a C-terminally hexahistidine-tagged $MopB_{HTH}$ fusion protein was transformed into *E. coli* BL21 (DE3) (Invitrogen). 2 l cultures were grown at 303 K in Luria–Bertani broth until an OD_{580} of 0.7 was reached. Over-expression of $MopB_{HTH}$ was induced by the addition of 0.5 m*M* IPTG. After further incubation for 3 h, the cells were harvested by centrifugation at 6000*g* and stored at 253 K.

Since $MopB_{HTH}$ precipitated under standard conditions, protein purification was optimized with regard to buffer composition and pH value. The best results were obtained using buffer *A* (5 m*M* MES, 5 m*M* CHES, 5 m*M* CAPSO, 10 m*M* NaH_2PO_4, 10 m*M* Tris–HCl pH 9.0, 100 m*M* NaCl) with 10 m*M* imidazole. The cell pellet was resuspended and cell disruption was performed using a French pressure cell (Thermo Scientific) at 13.8 MPa. After centrifugation at 277 K and 22 548*g* the lysate was further clarified using a 0.22 µm filter (Millipore). The lysate was applied onto an Ni–NTA chromatography column (Qiagen). The column was washed with two column volumes of buffer *A* containing 50 m*M* imidazole before the protein was eluted using buffer *A* containing 250 m*M* imidazole. Pooled protein-containing fractions were further purified by size-exclusion chromatography. For this purpose, fractions were applied onto a Superdex 75 HR 10/30 column (Amersham Biosciences) pre-equilibrated with buffer *B* (20 m*M* CHES, 100 m*M* NaCl pH 9.0). Separation was performed as described previously (Wiethaus *et al.*, 2009). $MopB_{HTH}$ eluted at 12.9 ml, which corresponds to a molecular weight of 26 kDa (Fig. 2*a*) and suggests that $MopB_{HTH}$ (like the full-length MopB protein) forms dimers. After pooling, proteins were concentrated using Amicon 15 kDa molecular-weight cutoff devices (Millipore), resulting in a final protein concentration of 15 mg ml^{-1}. The purity of $MopB_{HTH}$ was demonstrated by SDS–PAGE (Fig. 2*b*).

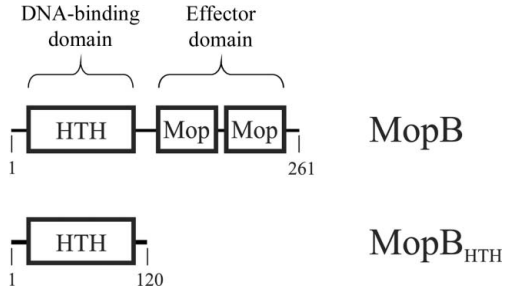

Figure 1
Domain organization of *R. capsulatus* full-length MopB and $MopB_{HTH}$. The DNA-binding domain harbours a helix–turn–helix (HTH) motif. The effector (Mo-binding) domain consists of two Mop subdomains. MopB and $MopB_{HTH}$ consist of 261 and 120 amino acids, respectively.

2.2. Functional analysis of $MopB_{HTH}$ by DNA mobility-shift assays

In order to test whether the isolated DNA-binding domain of MopB ($MopB_{HTH}$) was sufficient for target promoter binding, DNA mobility-shift assays were performed as described previously (Müller *et al.*, 2010). Briefly, a 209 bp ^{32}P-labelled *anfA* promoter fragment was incubated with increasing amounts of purified $MopB_{HTH}$ prior to separation of promoter–$MopB_{HTH}$ complexes from free promoter by polyacrylamide gel electrophoresis. Radioactively labelled bands were visualized using Amersham Hyperfilm MP (GE Healthcare). $MopB_{HTH}$ bound the *anfA* promoter (Fig. 2*c*), indicating that the isolated DNA-binding domain was correctly folded and active. $MopB_{HTH}$ bound the *anfA* promoter even more strongly than the full-length MopB protein (Müller *et al.*, 2010). As expected for a MopB protein lacking the Mo-binding effector domain, the affinity of $MopB_{HTH}$ for its target promoter was independent of Mo availability (Wiethaus *et al.*, 2006; data not shown).

2.3. Crystallization

Crystallization of $MopB_{HTH}$ was performed in 96-well format by applying the sitting-drop vapour-diffusion method at 291 K. Using a Phoenix crystallization robot (Art Robbins Instruments, Sunnyvale, USA), 0.1 µl $MopB_{HTH}$ solution was mixed with 0.1 µl of crystallization screening solutions (Qiagen). A single $MopB_{HTH}$ crystal was observed in JCSG+ Suite condition A6 [0.2 *M* lithium sulfate, 0.1 *M* phosphate/citrate pH 4.2, 20%(*w*/*v*) PEG 1000]. The trigonal crystal, with dimensions of about 50 × 50 × 25 µm (Fig. 3), was briefly soaked in mother liquor supplemented with 7.5% PEG 400 and 100 m*M* NaCl and flash-cooled in liquid nitrogen.

2.4. Data collection and processing

A data set was collected from a single crystal on beamline ID23-1 at the European Synchroton Radiation Facility (ESRF; Grenoble, France) using an ADSC Q315R CCD detector. The data were

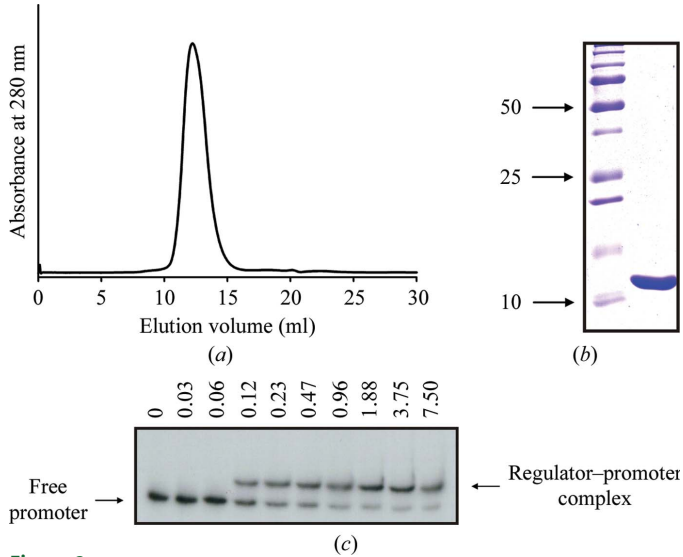

Figure 2
Purification of $MopB_{HTH}$ and DNA-binding assays. (*a*) $MopB_{HTH}$ eluted as a symmetric peak of 26 kDa indicating dimeric organization of the native protein. (*b*) $MopB_{HTH}$ appeared as a single band of ∼13 kDa after SDS–PAGE. Precision Plus Protein Standards All Blue (Bio-Rad) were used as molecular-mass standards. (*c*) Binding of $MopB_{HTH}$ to the *anfA* promoter was shown by DNA mobility-shift assays as described previously for the full-length MopB protein (Müller *et al.*, 2010). Increasing amounts (0–7.5 µ*M*) of $MopB_{HTH}$ were incubated with ^{32}P-labelled promoter.

Table 1
Data-collection statistics for $MopB_{HTH}$.

Values in parentheses are for the outermost resolution shell.

Wavelength (Å)	0.97625
Oscillation range (°)	1
Space group	$P3_121$ or $P3_221$
Unit-cell parameters (Å, °)	$a = b = 61.84$, $c = 139.64$, $\alpha = \beta = 90$, $\gamma = 120$
Resolution (Å)	42.49–3.3 (3.4–3.3)
Total reflections	51107
Unique reflections	8991
Multiplicity	10.1 (9.6)
$\langle I/\sigma(I)\rangle$	17.03 (4.23)
Completeness (%)	99.7 (99.3)
R_{merge}† (%)	6.9 (45.6)

† $R_{merge} = \sum_{hkl}\sum_i |I_i(hkl) - \langle I(hkl)\rangle| / \sum_{hkl}\sum_i I_i(hkl)$, where $I_i(hkl)$ is the intensity of an individual measurement and $\langle I(hkl)\rangle$ is the corresponding mean value.

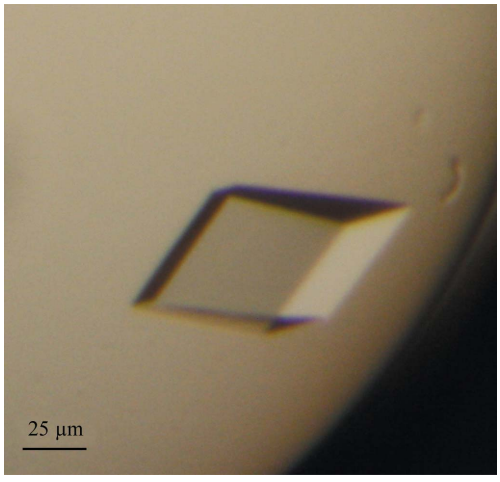

Figure 3
Trigonal crystal of $MopB_{HTH}$. Crystallization was performed in 0.2 *M* lithium sulfate, 0.1 *M* phosphate/citrate pH 4.2, 20%(*w*/*v*) PEG 1000.

obtained to a resolution of 3.3 Å at 100 K using a wavelength of 0.97625 Å. The data set consisted of 180 frames with an oscillation range of 1°. It was integrated with *XDS* (Kabsch, 2010) and scaled using *XSCALE* (Kabsch, 2010). The statistics of the resulting data are shown in Table 1.

3. Results and discussion

The isolated DNA-binding domain of MopB ($MopB_{HTH}$) was successfully expressed in *E. coli* with a hexahistidine tag and purified *via* Ni–NTA and size-exclusion chromatography (Figs. 1 and 2). DNA mobility-shift assays with purified $MopB_{HTH}$ showed that the isolated DNA-binding domain was sufficient for promoter binding (Fig. 2). $MopB_{HTH}$ was crystallized using the sitting-drop vapour-diffusion method at 291 K. After 25 d, a diffracting crystal with dimensions of 50 × 50 × 25 µm was obtained (Fig. 3). A data set was collected from a single crystal on beamline ID23-1 at the European Synchroton Radiation Facility (ESRF; Grenoble, France). After scaling, the data were 99.7% complete to 3.3 Å resolution, with an overall R_{merge} of 6.9%.

The crystal belonged to the trigonal space group $P3_121$ or $P3_221$. A Matthews coefficient of 2.96 $Å^3\,Da^{-1}$ was estimated, assuming the presence of two molecules per asymmetric unit, with a solvent content of 58.54%, which is consistent with a dimeric organization of $MopB_{HTH}$ as determined by size-exclusion chromatography (Fig. 2). In both cases a twin fraction of 0.02–0.3 corresponding to the twin law $(-h, -k, l)$ was estimated using the merohedral twinning server (Yeates, 1997), *phenix.xtriage* (Zwart *et al.*, 2005) or *TRUNCATE* (French & Wilson, 1978).

Molecular replacement of $MopB_{HTH}$ was performed using the structures of the molybdate-dependent transcriptional regulator ModE from *E. coli* (PDB entries 1b9n and 1o7l; Hall *et al.*, 1999; Schüttelkopf *et al.*, 2003) and a putative ModE from *Agrobacterium tumefaciens* (PDB entry 2ijl; Midwest Center for Structural Genomics, unpublished work). Molecular-replacement searches were executed for all possible space groups. No clear solution could be identified. Therefore, we are currently attempting to solve the structure of $MopB_{HTH}$ using both the MIR method with heavy-atom soaks and sulfur single anomalous dispersion.

We thank the beamline staff of ID23-1 at the ESRF (Grenoble, France) for support during data collection, Petros Sarantopoulos for excellent technical support, Sandra Neumann for plasmid construction and Franz Narberhaus for continuous support. This work was supported by grants from the Deutsche Forschungsgemeinschaft (Ma 1814/3-3) to BM and from the Ruhr University Research School to AM.

References

Anderson, L. A., Palmer, T., Price, N. C., Bornemann, S., Boxer, D. H. & Pau, R. N. (1997). *Eur. J. Biochem.* **246**, 119–126.
Bender, R. A. (2010). *J. Bacteriol.* **192**, 4801–4811.
Cao, H., Krishnan, G., Goumnerov, B., Tsongalis, J., Tompkins, R. & Rahme, L. G. (2001). *Proc. Natl Acad. Sci. USA*, **98**, 14613–14618.
French, S. & Wilson, K. (1978). *Acta Cryst.* A**34**, 517–525.
Hall, D. R., Gourley, D. G., Duke, E. M. H., Leonard, G. A., Anderson, L. A., Pau, R. N., Boxer, D. H. & Hunter, W. N. (1999). *Acta Cryst.* D**55**, 542–543.
Kabsch, W. (2010). *Acta Cryst.* D**66**, 125–132.
Kutsche, M., Leimkühler, S., Angermüller, S. & Klipp, W. (1996). *J. Bacteriol.* **178**, 2010–2017.
Maddocks, S. E. & Oyston, P. C. (2008). *Microbiology*, **154**, 3609–3623.
Madigan, M. (1995). *Anoxygenic Photosynthetic Bacteria*, edited by R. Blankenship, M. Madigan & C. Bauer, pp. 915–928. Dordrecht: Kluwer Academic Publishers.
Masepohl, B. & Hallenbeck, P. C. (2010). *Adv. Exp. Med. Biol.* **675**, 49–70.
Monferrer, D., Tralau, T., Kertesz, M. A., Dix, I., Solà, M. & Usón, I. (2010). *Mol. Microbiol.* **75**, 1199–1214.
Müller, A., Püttmann, L., Barthel, R., Schön, M., Lackmann, J.-W., Narberhaus, F. & Masepohl, B. (2010). *FEMS Microbiol. Lett.* **307**, 191–200.
Muraoka, S., Okumura, R., Ogawa, N., Nonaka, T., Miyashita, K. & Senda, T. (2003). *J. Mol. Biol.* **328**, 555–566.
Parsek, M. R., Ye, R. W., Pun, P. & Chakrabarty, A. M. (1994). *J. Biol. Chem.* **269**, 11279–11284.
Russell, D. A., Byrne, G. A., O'Connell, E. P., Boland, C. A. & Meijer, W. G. (2004). *J. Bacteriol.* **186**, 5576–5584.
Schell, M. A. (1993). *Annu. Rev. Microbiol.* **47**, 597–626.
Schlaman, H. R., Okker, R. J. & Lugtenberg, B. J. (1992). *J. Bacteriol.* **174**, 5177–5182.
Schüttelkopf, A. W., Boxer, D. H. & Hunter, W. N. (2003). *J. Mol. Biol.* **326**, 761–767.
Viale, A. M., Kobayashi, H., Akazawa, T. & Henikoff, S. (1991). *J. Bacteriol.* **173**, 5224–5229.
Wiethaus, J., Müller, A., Neumann, M., Neumann, S., Leimkühler, S., Narberhaus, F. & Masepohl, B. (2009). *J. Bacteriol.* **191**, 5205–5215.
Wiethaus, J., Wirsing, A., Narberhaus, F. & Masepohl, B. (2006). *J. Bacteriol.* **188**, 8441–8451.
Yeates, T. O. (1997). *Methods Enzymol.* **276**, 344–358.
Zaim, J. & Kierzek, A. M. (2003). *Nucleic Acids Res.* **31**, 1444–1454.
Zwart, P., Grosse-Kunstleve, R. W. & Adams, P. D. (2005). *CCP4 Newsl.* **43**, contribution 7.